

An electron motion induced by magnetic field pulse in bi-layer quantum wire

T. Chwiej*

AGH University of Science and Technology, al. A. Mickiewicza 30, 30-059 Cracow, Poland

We consider theoretically the possibility of an electron acceleration in quantum wire by short magnetic pulses lasted between several to few tens of picoseconds. We show that such possibility exists provided that, the electron is initially localized in part of nanowire that consists of two vertically aligned layers which are tunnel coupled. When a horizontally directed magnetic field, changeable in time, is also perpendicular to the main axis of a wire, it generates a rotational electric field in it which pushes the upper and the lower parts of the electron wavepacket in opposite directions. We have found however, that for an asymmetric vertical confinement, the majority part of charge density starts to move in the direction of local electric field in its layer but it also drags the minority part in the same direction what results in coherent motion of an entire wavepacket. We discuss the dynamics of this motion in dependence on the time characteristics of the magnetic pulse.

PACS numbers: 72.25.Dc, 73.21.Hb

Keywords: quantum wire, ballistic transport, magnetic field

I. INTRODUCTION

The tunnel coupling between two quantum wires has a great impact on the single electron transport properties.¹⁻⁵ If magnetic field penetrates such quantum system it can modify the magnitude of a tunnel coupling but the extent of such modifications depends on the magnetic field strength and mutual arrangement of magnetic field and the wire axis.^{6,7} If magnetic field is parallel to the wire axis, it squeezes the wavefunctions of magneto-subbands within each layer what results in lower value of a tunnel factor.^{7,8} On the other hand, if it is set perpendicularly to wire axis and to the layers coupled laterally or vertically, it can hybridize the magnetosubbands between layers. This modifies, to a large extent, the energy dispersion relation $E(k)$ since the pseudo-gaps are opened and the negative dispersion relation appear in energy spectrum.^{3,9} As we have shown in our last paper, hybridization which leads to formation of pseudogaps can be utilized for tuning the magnitude of spin polarization of wire's conductance provided that the wire has low density of defects.¹⁰

In present paper we study the dynamics of an electron motion in a bi-layer quantum wire made of InGaAs/GaAs and GaAs/AlGaAs heterostructure which motion is induced by the magnetic pulse only. Magnetic acceleration or deceleration of an electron in such nanostructure can be conducted provided that: i) the wave functions originated from different layers are mutually hybridized, and, ii) the time duration of magnetic pulse is between a few and tens of picoseconds. At present, such short magnetic pulses can be generated by using the Auston's photoconductive switches^{11,12} or by the off-resonant magnetization of ferromagnetic thin films with the terahertz laser pulses.¹³ Due to the Maxwell law i.e. $\partial \vec{B}/\partial t = -\nabla \times \vec{E}$, if the time varying magnetic field is directed perpendicularly to a wire's axis as well as to the vertically aligned transport layers, it generates the rotational electric field which try to push two parts of the electron wavepacket being localized in both layers in the opposite directions.

The action of temporary rotational electric field on the electron wavepacket confined in vertical bi-layer nanowire is schematically depicted in Fig.1. We have investigated this mechanism of acceleration of an electron in nanostructure of this kind and have found that the asymmetry introduced to the vertical confinement enables an entire electron wavepacket to move in a particular direction but its further dynamics, i.e. after the pulse is finished, depends mainly on the time length of magnetic pulse and on that, whether the magnetic field finally vanishes or its value remains non-zero but is fixed for further times. In the latter case, which is an analog of switching the magnetic field on, the electron motion in constant magnetic field is governed by the magnetic force which for longer times breaks the coherence between the upper and lower layers' parts of an electron wavepacket.

Paper is organized as follows. In Sec.II we present numerical model of solving the time-dependent Schrödinger equation for an electron confined in bi-layer nanowire, results of simulations are presented and discussed in Sec.III. We end up considerations with conclusions given in Sec.IV.

II. THEORETICAL MODEL

We start our considerations with the single electron Hamiltonian $\hat{H} = (\hat{\mathbf{p}} + e\mathbf{A})^2/2m^* + V_c(\mathbf{r})$. Throughout the paper we will use the time-dependent vector potential in non-symmetric form $\mathbf{A}(t) = [zB(t), 0, 0]$ which gives the magnetic field piercing the layers horizontally $\mathbf{B} = [0, B(t), 0]$ and being perpendicular to the direction of an electron motion. We assume an electron can move along the wire axis in x direction within the harmonic oscillator potential ($V_1(x) = m^*\omega^2 x^2/2$) and can tunnel between two vertical layers which establish a double-well potential in z direction ($V_2(z)$). Its motion in y direction is frozen to the ground state, and is neglected in further discussion. Sketch of a model confinement potential is shown in Fig.1. Based on these as-

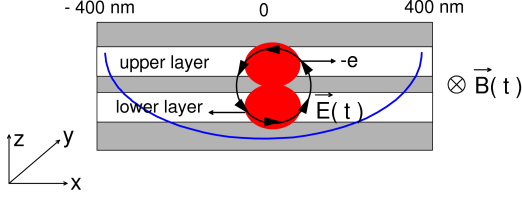


FIG. 1: (Color online) The cross-section of a model bi-layer nanowire considered in paper. The electron motion in x direction within harmonic oscillator potential (blue line) is stimulated by rotational electric field to be induced by the time varying magnetic field which is pointed along y direction, and, provided that both, upper and lower layers are tunnel coupled.

sumptions, and additionally assuming that the confinement potential in x and z directions is separable that is $V_c(x, z) = V_1(x) + V_2(z)$, we make the problem simpler diagonalizing the part of Hamiltonian dependent on z variable only $\hat{h}_z = -(\hbar^2/2m^*)\partial/\partial z^2 + V_2(z)$. From the set of its all eigenstates $f_k(z)$ we chose only two lowest eigenmodes to form the functions basis $\{f_1, f_2\}$. The rest lie much higher on energy scale and therefore their contributions to final solution are neglected. Next, calculating the matrix elements of Hamiltonian in this basis $\hat{H}_{k,k'} = \langle f_k | \hat{H} | f_{k'} \rangle$ we get:

$$\begin{aligned} \hat{H}_{k,k'} = & \left(\hat{T}_x + V_1(x) + E_k^{(z)} \right) \delta_{k,k'} \\ & + \hbar\omega_c Z_{k,k'}^{(1)} \hat{k}_x + \frac{m^* \omega_c^2}{2} Z_{k,k'}^{(2)} \end{aligned} \quad (1)$$

where \hat{T}_x is kinetic operator for x direction, $E_k^{(z)}$ is a k-th eigenenergy of Hamiltonian \hat{h}_z , $\omega_c = eB/m^*$ is the cyclotron frequency, matrix elements $Z_{k,k'}^{(1)}$ and $Z_{k,k'}^{(2)}$ are defined as $Z_{k,k'}^{(m)} = \langle f_k | z^m | f_{k'} \rangle$ and $\hat{k}_x = \hat{p}_x/\hbar = -i\partial/\partial x$. Hamiltonian given in Eq.1 depends on time through the second and the third terms in above equation which include ω_c because magnetic field change its value during an evolution of quantum system. This form of energy operator allows us to define the wave function of an electron as a two-component object $|\Psi(x, t)\rangle = \sum_{k=1}^2 \psi_k(x, t) |f_k\rangle$ for which the effective time-dependent Schrödinger equation has the following form:

$$i\hbar \frac{\partial}{\partial t} \begin{bmatrix} \psi_1(x, t) \\ \psi_2(x, t) \end{bmatrix} = \begin{bmatrix} H_{11} & H_{12} \\ H_{21} & H_{22} \end{bmatrix} \begin{bmatrix} \psi_1(x, t) \\ \psi_2(x, t) \end{bmatrix} \quad (2)$$

with matrix elements $H_{k,k'}$ defined by Eq.1.

To describe the confinement in vertical direction within two layers we use the following approximation^{5,14}:

$$V_2(z) = V_{max} \{ \sin[(1 + z/b)\pi/2] + \alpha \sin[\pi(1 + z/b)] \} \quad (3)$$

which is symmetric for $\alpha = 0$ and the upper layers becomes deeper than the lower one for $\alpha > 0$. The latter case is studied in detail in next section. The shape of $V_2(z)$ has a great impact on the dynamics of an electron

in quantum wire. For $\alpha = 0$, basis wave functions $f_1(z)$ and $f_2(z)$ have defined parities. Then, the third term in Eq.1 disappears and only the second term mixes both components $\psi_1(x)$ and $\psi_2(x)$ of an electron's wave function through the off-diagonal elements H_{12} and H_{21} in Eq.2 as the first term is pure diagonal. On the other hand, when $\alpha > 0$, the third term in Eq.1 also gives contribution to off-diagonal elements in Eq.2 and to the diagonal ones as well. Mixing of these components is crucial for inducing the motion of an electron by the magnetic field pulse. If there is no mixing during the time evolution, the electron permanently occupy the lowest state that is $\psi_1(x, t)$ whereas occupation of $\psi_2(x, t)$ has to be zero due to the condition $E_1^{(z)} < E_2^{(z)}$, otherwise, mixing of these elements should change the dynamics of an electron in the wire. According to the definitions of the off-diagonal elements given by the second and third terms in Eq.1, the mixing takes place only when $B \neq 0$ that is during the magnetic pulse ($\partial B/\partial t \neq 0$) or for constant magnetic field but provided that an electron moves within the wire.

Even though, the last two terms in Eq.1 can mix the wave functions $\psi_1(x)$ and $\psi_2(x)$, only the second term may force an electron to change its position. The proof is straightforward. First, consider the ground state of electron for $B = 0$, its wave function at $t = 0$ is given then by $\Psi(x, t) = [\psi_1(x, 0), \psi_2(x, 0)] = [g_0(x), 0]$, with $g_0(x)$ being the normalized square integrable function. If we now skip in Hamiltonian in Eq.2 the term $\hbar\omega_c Z_{k,k'}^{(1)} \hat{k}_x$ and replace the time derivative with the forward first-order finite difference formula, we obtain in first time step an approximated expressions for: i) $\psi_1(x, \Delta t) = (1 - i\Delta t m^* \omega_c^2 E_1/\hbar) \psi_1(x, 0)$, where E_1 is the total energy of electron at $t = 0$ and the contribution from ψ_2 vanishes since $\psi_2(x, 0) = 0$, and, ii) $\psi_2(x, \Delta t) = -(i\Delta t m^* \omega_c^2 Z_{21}^{(2)}/2) \psi_1(x, 0)$. In other words, part of $g_0(x)$ is moved from ψ_1 to ψ_2 and vice versa for further time steps but the shape of $|\Psi(x, t)|^2$ is retained in any further time instant. Simply, this Hamiltonian term is a diamagnetic energy shift which is responsible for optimizing the wave function shape in z direction that is for its stronger localization in magnetic field. The dynamics of an electron during the time of simulation is governed by the term $\hbar\omega_c Z_{k,k'}^{(1)} \hat{k}_x$ which includes the derivative over x variable.

We simulate the motion of an electron in bi-layer nanowire stimulated by the magnetic field pulse by finding the solution of time-dependent Schrödinger equation [Eq.2] in subsequent time instants by means of 4-th order Runge-Kutta method with time step $\Delta t = 10^{-4}$ ps. For this purpose we have performed a set of numerical simulations on regular mesh of nodes in x direction. We limit the length of quantum wire to 800 nm and impose smooth confining potential in this direction as for the quantum oscillator $V_1(x) = m^* \omega_0^2 x^2/2$ with oscillator strength $\hbar\omega_0 = 0.5$ meV. This spatial constriction allows us to study of an electron motion for quite long times after the

magnetic pulse is finished what is particularly important if an influence of magnetic force ($B_y = \text{const}$) on the coupling strength between the upper and lower parts of electron's wavepacket is taken into account. The basis functions $\{f_1(z), f_2(z)\}$ were also found numerically with finite difference method after discretization of Hamiltonian \hat{h}_z on spatial mesh with 200 nodes for z direction. The number of nodes in x direction was set to 400. All simulations were preceded by diagonalization of Hamiltonian appearing in Eq.2 to prepare the starting wavepacket for $t = 0$ i.e. to find $\Psi(x, t = 0) = [\psi_1(x, 0), \psi_2(x, 0)]$.

Value of parameter b which defines the extent of vertical confinement in Eq.3 was equal 30 nm. The height of tunnel barrier between the upper and lower layers depends on magnitude of V_{max} . We set its value equal to 150 meV for which the energy splitting between the bounding (f_1) and the antibounding (f_2) basis states equals $E_{21}^{(z)} = E_2^{(z)} - E_1^{(z)} = 2$ meV for symmetric confinement ($\alpha = 0$). When α becomes non-zero then $\Delta E_{21}^{(z)}$ grows what eventually lowers the extent of mixing ψ_1 and ψ_2 components of an electron's wave function. This can not be however omitted since for $\alpha = 0$, the wavepackets localized in symmetric layers move in opposite directions [see Fig.1] and an electron wavepacket motion as a whole, in an arbitrarily chosen direction, can be obtained only for $\alpha > 0$ what will be shown below. In paper we consider two cases, in first the electron is accelerated by single magnetic pulse, while in second, its motion is induced when the magnetic field is switched on/off.

III. RESULTS

A. Acceleration of an electron by a single magnetic pulse

We start presentation of our results for a case the electron is accelerated by a single magnetic pulse defined as: $B(t) = B_m \sin(\pi t/t_{imp}) \cdot \Theta(t) \cdot \Theta(t_{imp} - t)$, where $\Theta(t)$ is the Heaviside step function, the amplitude of magnetic field equals $B_m = 5$ T and the time duration of a pulse is changed within the range $t_{imp} = 5 - 50$ ps.

Figure 2(a) shows the time variations of the electron positions in the upper and in the lower layers obtained according to Eqs. (5) and (6) [see description below] for symmetric bi-layer nanowire ($\alpha = 0$). The magnetic pulse starts at $t = 0$ and ends at $t = 20$ ps. Within this time interval, the parts of electron wavepacket localized in upper and in lower layers oscillate in x direction but with opposite phases i.e. the upper part starts to move to the right while the second one, localized in the lower layer, to the left, and then, both change the directions of their motions three times due to reflections within the regions of high confining potential. After the magnetic field eventually vanishes, these oscillations are strongly damped but do not disappear entirely. The inset in Fig.2(a) shows that even though for $t > t_{imp}$ the amplitude of these oscillations become very small but

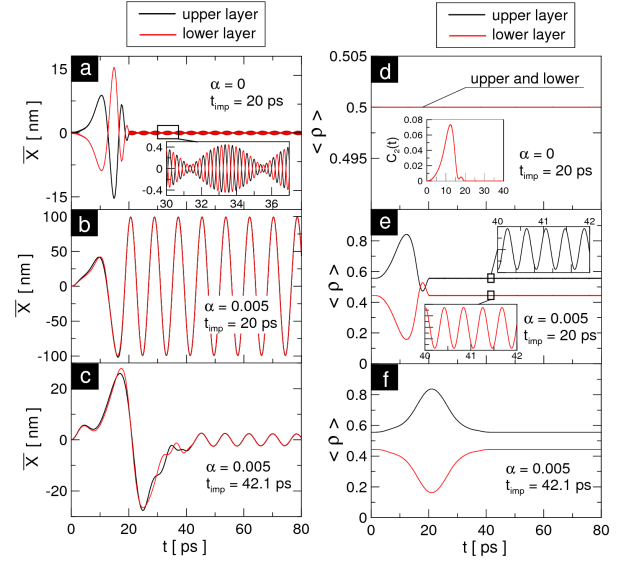


FIG. 2: (Color online) Expectation value of electron position (left column) and the density (right column) localized in the upper (red color) and in the lower layer (black color) during the time of simulation for $\alpha = 0$ (first row) and $\alpha = 0.005$ (second and third rows). Inset in figures (a) and (e) shows zooms of oscillations of \bar{x} and $\langle \rho \rangle$ remained after the magnetic pulse is ended. The inset in (d) shows $C_2 = \langle \psi_2 | \psi_2 \rangle$ that is an occupation of second eigenstate for vertical quantization. Calculations were performed for parameters: $m^* = 0.04$ (InGaAs) and $\Delta E_{21}^z = 9.83$ meV (a) and $\Delta E_{21}^z = 9.9$ meV in (b) and (c).

oscillations remain stable for longer times. The beating pattern shown in this inset come into existence due to the overlap of two kinds of oscillations, one with period equal to $T_1 = 8.3$ ps and second with period $T_2 = 0.44$ ps. To determine their origin we first calculated the expectation value of electron position in upper layer according to formula $\langle x \rangle_{z>0} = \langle \Psi | x \cdot \Theta(z) | \Psi \rangle$. Exactly at the moment the magnetic pulse ends ($B = 0$), the electron wave function can be expressed as $\Psi(x, y, z, t = t_{imp}) = \sum_k \psi_k(x, t_{imp}) f_k(z) g_0(y)$. The part of wave function which is dependent on x variable was expanded within the base constituted by Hermite polynomials i.e. the quantum oscillator eigenstates Φ_μ :

$$\Psi(x, y, z, t) = \sum_k \sum_\mu d_{k,\mu} \Phi_\mu(x) \cdot f_k(z) g_0(y) e^{-i(E_\mu^x + E_k^z + E_0^y)t/\hbar} \quad (4)$$

In above equation, $d_{k,\mu}$ are the linear combination coefficients, $\Phi_\mu(x) = C_\mu H_\mu(x) e^{-x^2}$ are the normalized Hermite polynomials while three arguments appearing in phase factor are the eigenenergies for quantized motion of electron in x (E_μ^x), y (E_0^y) and z (E_k^z) directions. According to this definition, the position of electron in an upper layer (dependence on $g_0(y)$ and E_0^y) disappear after

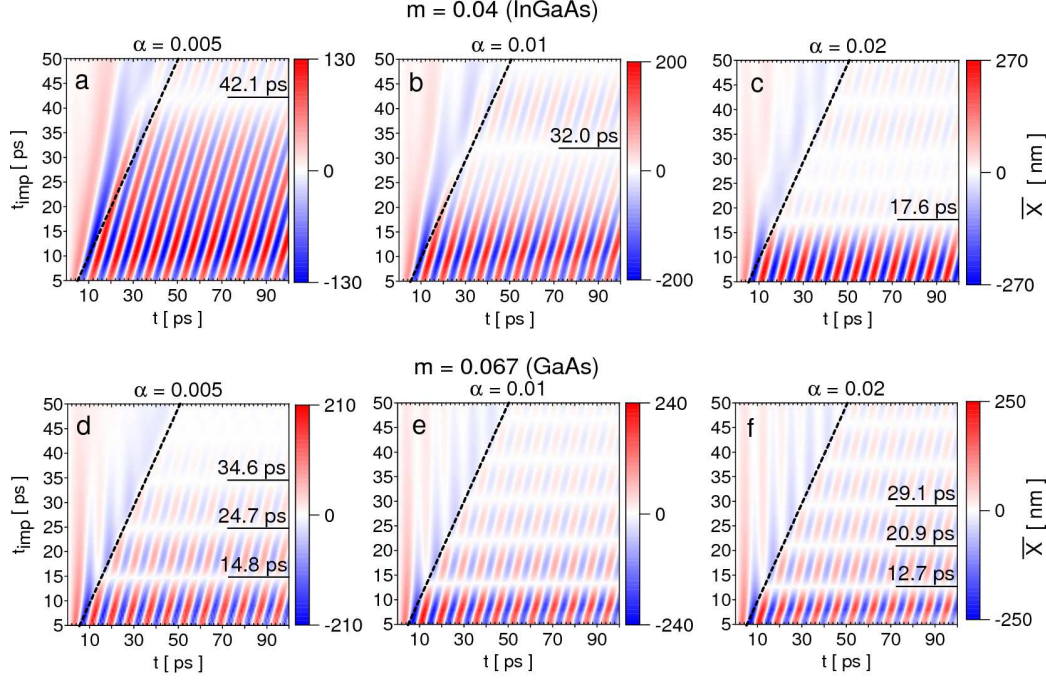


FIG. 3: (Color online) Dependence of the normalized expectation value of electron position (\bar{x}) in bi-layer quantum wire on time length of magnetic pulse and on the time of simulation. The inclined dashed lines mark the right border of magnetic field pulse. The upper row displays the results obtained for InGaAs and effective mass $m_{InGaAs}^* = 0.04$ while the lower one for GaAs and effective mass $m_{GaAs}^* = 0.067$. Parameter α which is shown on top of each subfigure represents an actual asymmetry in vertical confinement.

integration over y variable) reads:

$$\langle x \rangle_{z>0} = \sum_{k,m} \sum_{\mu,\nu} d_{k,\mu}^* d_{m,\nu} \langle \Phi_\mu | x | \Phi_\nu \rangle \langle f_k | \Theta(z) | f_m \rangle \times e^{i\Delta E_{\mu,\nu}^x t/\hbar} e^{i\Delta E_{k,m}^z t/\hbar} \quad (5)$$

Since the amounts of probability density gathered in both layers may differ from unity we normalized the expectation value of electron position in upper (or lower) layer:

$$\bar{x}_{z>0} = \frac{\langle x \rangle_{z>0}}{\langle \Psi | \Psi \rangle_{z>0}} \quad (6)$$

The matrix elements $\langle \Phi_\mu | x | \Phi_\nu \rangle$ have non-zero values only if $\mu = \nu \pm 1$ that is for $\Delta E_{\mu,\nu} = \pm \hbar \omega_0$ and the coupling of these non-diagonal terms are responsible for the appearance of oscillations with longer period $T_1 = \hbar / \Delta E_{\mu,\mu\pm 1} = 8.3$ ps, provided that, ΔE_{km}^z vanishes for $k = m$ in Eq.5. Otherwise, when conditions $k \neq m$ and $\mu = \nu \pm 1$ are fulfilled then the total phase factor oscillates with period dependent on the sum of both energy differences i.e. $\Delta E = \Delta E_{21}^z + \hbar \omega_0 = 10.33$ meV what gives the period equal to $T_2' = 0.44$ ps. However this value is very close to value $T_2 = \hbar / \Delta E_{21}^1 = 0.42$ ps what means that the coupling between vertical layers [due to the terms $\langle f_k | \Theta(\pm z) | f_m \rangle$] is the main source of high frequency oscillations visible in the inset in Fig.2(a). Equation 5 can be further employed for calculation of

$\langle \rho \rangle_{z>0}$ if the terms $\langle \Phi_\mu | x | \Phi_\nu \rangle$ will be substituted by $\langle \Phi_\mu | \Phi_\nu \rangle = \delta_{\mu,\nu}$. This substitution eliminates dependence of total phase on $\Delta E_{\mu,\nu}^x = 0$ but leaves it still dependent on $\Delta E_{k,m}^z$ value. However in Fig.2(d) there are no oscillations at any time instant. For $\alpha = 0$, the amounts of electron density confined in both layers are equal, simply due to the symmetry constriction imposed on the confining potential [see Fig.2(d)].

When $\alpha > 0$ and the confinement energy in lower layer becomes higher than the one in an upper layer, then for $t = 0$ the larger part of electron density is gathered in upper layer [see Figs.2(e) and (f)]. Therefore, when magnetic field starts to grow, the majority of wavepacket move to right but this time the rest of wavepacket is also pulled into this direction. In Figs. 2(b) and 2(c) we see that both densities move synchronously and independently on the time duration of magnetic pulse. Due to an asymmetry that has been introduced into the confining potential in vertical direction, the amounts of electron densities in both layers are smoothly changed when $\partial B / \partial t \neq 0$ and for $t > t_{imp}$ become fixed [Figs. 2(e) and 2(f)] besides the small oscillations for frequency $\omega_2' = 2\pi / T_2'$ visible in the inset in Fig.2(e). The length of magnetic pulse has great impact on the amplitude of the electron oscillation within quantum wire. For $t_{imp} = 20$ ps the amplitude of expectation value of electron position in wire reaches even $\bar{x}_{max} = 100$ nm while for two times longer pulse the amplitude of electron oscil-

lations falls to value $\bar{x}_{max} = 2.3$ nm. Despite the different lengths of these magnetic pulses, the period of oscillations in both cases is the same and equals $T_1 = 8.3$ ps that is the dynamics of wavepacket is governed by the energy levels structure of quantum harmonic oscillator established in x direction.

Analysis of the results showed in Fig.2(a-c) allows us to make a statement that the characteristics of the electron motion induced by magnetic pulse in quantum bi-layer wire is dependent on at least two factors: i) the time length of a magnetic pulse, and, ii) the degree of asymmetry in vertical confinement provided that the amplitude of magnetic field is fixed. In order to study the influence of these factors on dynamics of electron motion in the wire we computed the expectation value of the electron position as function of t_{imp} length and on the time of simulation. Results for effective mass $m^* = 0.04$ (InGaAs) are presented in first row in Fig.3 for $\alpha = 0.005, 0.01, 0.02$. These α 's values give the energy splittings between two lowest eigenstates in vertical direction equal to $\Delta E_{21}^z = 9.9$ meV, 10.1 meV and 10.9 meV. For comparison, second row in this figure displays the results for $m^* = 0.067$ (GaAs) and for the energy splittings $\Delta E_{21}^z = 2.3$ meV, 3.1 meV and 5.1 meV. If an electron effective mass is small [first row in Fig.3] then the increase of a confining potential asymmetry brings two main effects. First, the amplitude of \bar{x} grows [compare the ranges of color scales in Figs.3(a-c)] if value of α is increased. For example, for $\alpha = 0.005$ the amplitude of electron oscillations in x direction reaches $\bar{x}_{max} = 130$ ps while for $\alpha = 0.02$ it becomes two times larger. Second, the time length of magnetic pulse which allows to obtain significant amplitudes systematically decreases for larger α 's values. For $\alpha = 0.005$ the electron motion in quantum wire can not be induced by pulses longer than 42.1 ps while for $\alpha = 0.02$ it is limited only to 17.6 ps. For longer pulses, oscillations are still possible but they might have much smaller amplitudes.

For larger effective mass [second row in Fig.3] the upper limit for the time length of magnetic pulse which still may induce large oscillations of electron position in bi-layer nanowire is lowered to several picoseconds but its sensitivity to potential asymmetry is not so high as in the previous case. Now, its value decreases from 14.8ps to 12.7 ps when the value of α increases from 0.005 to 0.02. On the other hand, the largest amplitude of electron oscillations becomes less dependent on potential asymmetry for heavier particle, the change of α 's value from 0.005 to 0.02 increases the amplitude of \bar{x} from 210 nm to 250 nm that is in a three times thinner range than for the smaller effective mass.

B. Electron motion induced by switching the magnetic field on/off

In this section we present the results obtained for a pulse generated by switching the magnetic field on/off

which is modelled in our simulations by following formula:

$$B(t) = B_m \sin(2\pi t/t_{imp} + \beta\pi/2) \cdot \Theta(t) \cdot \Theta(t_{imp} - t) + \gamma \cdot B_m \cdot \Theta(t - t_{imp}) \quad (7)$$

where: $\beta = 0$ and $\gamma = 1$ stand for the magnetic field growing in time [$\partial B/\partial t > 0$ for $t \leq t_{imp}$] from 0 to B_m while $\beta = 1$ and $\gamma = 0$ for vanishing field [$\partial B/\partial t < 0$ for $t \leq t_{imp}$] from B_m to 0.

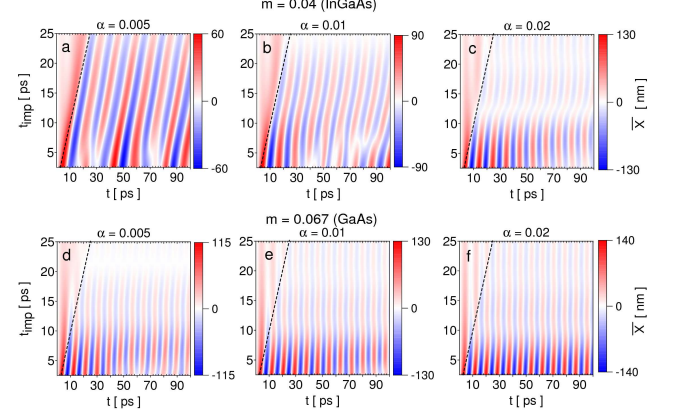


FIG. 4: (Color online) Normalized expectation value of an electron position (\bar{x}) in an upper layer depending on the time interval the magnetic field is switched on [$\partial B/\partial t > 0$ for $t < t_{imp}$] and the time of simulation. Other parameters are given on the top of each figure.

Results for the first case, when magnetic field is turned on, are presented in Fig.4. For InGaAs bi-layer wire, the dynamics of an electron changes qualitatively and quantitatively much as the imbalance in the confining potential in the upper and in the lower layers raises [cf. Figs. 4(a-c)]. For $\alpha = 0.005$ and $\alpha = 0.01$ the pattern of \bar{x} is very irregular for short pulses ($t < 10$ ps) and becomes regular that is with distinct single period of oscillations for longer pulses. However, it does not concern the case with $\alpha = 0.02$ [Fig.4(c)] for which we may single out one main period being the same for all values of t_{imp} . To explain the reasons of this irregularity we will analyze the changes in \bar{x} and in $\langle \rho \rangle$ in both layers for $t_{imp} = 5$ ps, $\alpha = 0.005$ and $m^* = 0.04$. Results are shown in Figs.5(a) and (b).

In Fig.5(a) we see that the time characteristics of \bar{x} for both parts of wavepacket is similar for $t < 24.2$ ps but thereafter their motions become decoupled even though the density may still flow between the layers [Fig.5(b)]. At $t = 0$ the electron is at rest in the center of nanowire [Fig.5(c)] and when the magnetic field starts raising the rotational electric field is generated with opposite directions in upper and lower layers. The upper layer confines a majority of electron density which begins to move to the right according to the electric field. Simultaneously, it pulls the minority of density in this direction but against the x-component of electric field in a lower

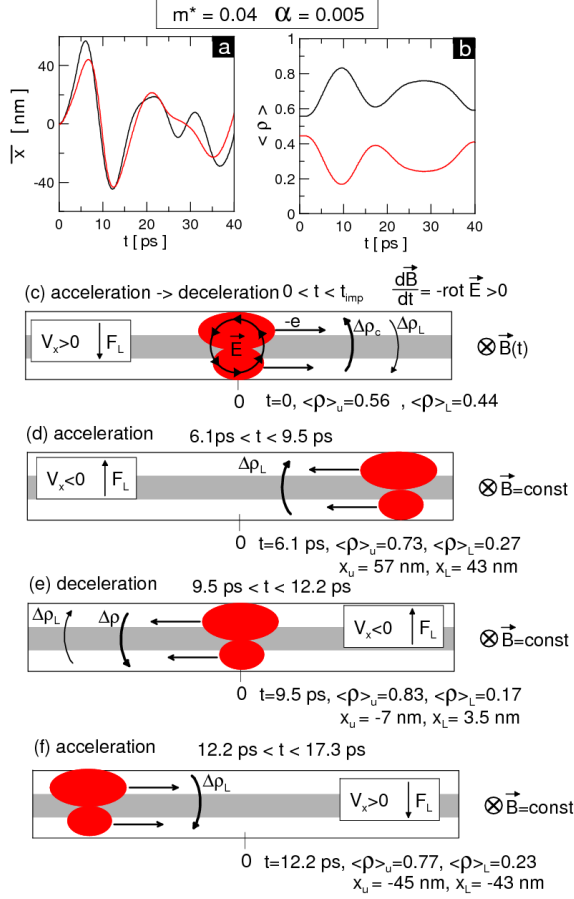


FIG. 5: (Color online) The time variations of the expectation value of electron position (a) and of the electron density in the upper and in the lower layers (b) for $t_{imp} = 5$ ps and for magnetic field being switched on. Black and red colours in (a) and (b) mark the results for the upper and lower layers, respectively. $\Delta\rho_c$ shows the density flow direction caused by the stronger localization in the upper layer, $\Delta\rho_L$ indicate the density flow due to magnetic force while $\Delta\rho$ marks the density flow caused by its unbalanced accumulation in layers.

layer. Even though the motion to the right implies the magnetic force is directed downwards to the lower layer, in fact, density flows upwards since the raising magnetic field enhances localization of density in deeper, the upper well, for $t < 5$ ps. Then the strength of magnetic field is fixed ($B = \text{const}$) and for time instant $t = 6.1$ ps the wavepacket is stopped and after that turned back due to its reflection of the high confinig potential on the right side [Fig.5(d)]. In the next stage the electron moves to the left, first being accelerated ($6.1 \text{ ps} < t < 9.5 \text{ ps}$) and next when it passes the center of nanowire ($x = 0$) being decelerated ($9.5 \text{ ps} < t < 12.2 \text{ ps}$). Since the magnetic field is still applied to the system, the direction of magnetic force is now reversed [see Figs. 5(d) and 5(e)] what forces an additional part of electron density to flow from lower to upper layer what we notice in Fig.5(b). At time in-

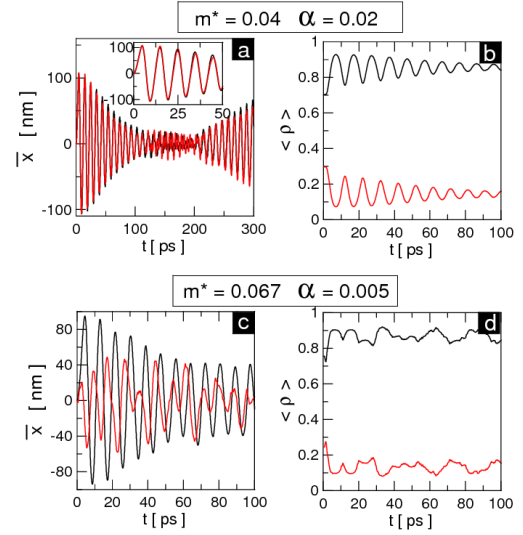


FIG. 6: (Color online) The time changes of expectation values of electron positions (a,c) and of the densities (b,d) in the upper and in the lower layers for $t_{imp} = 5$ ps when magnetic field is turned on. Black and red colors mark the results for an upper and for a lower layer, respectively. Values of α and of the effective masses are given on top of first and second row.

stant $t = 12.2$ ps the decelerated motion of electron is stopped on the left side of the nanowire and next the directions of electron wavepacket motion and of magnetic force are again reversed. For the right directed motion, the Lorentz force now easily shifts the part of density from the upper to lower layer. Thus, the existence of magnetic force is crucial for the dynamics of the electron motion in bi-layer nanosystem because when the electron oscillates between the left and right turning points, the density may flow between layers but with vertical velocities what eventually hinders the upper and lower parts of an electron wavepacket. For that reason the electron motion is constantly slowing down on average and both parts of wavepacket, the upper and the lower ones, start to oscillate along x axis in asynchronous manner for $t > 24.2$ ps [Fig.5(a)].

If the vertical confinement becomes more asymmetric ($\alpha = 0.02$) or the effective mass is getting larger ($m^* = 0.067$) then an asynchronous motions of the upper and lower electron densities also appear [see Figs. 6(a) and 6(c)]. In this case however, the disproportion between the amounts of densities gathered in layers is significantly larger e.g. $\langle \rho \rangle_{up} = 0.7$ and $\langle \rho \rangle_{lo} = 0.3$ for $t = 0$ for $m^* = 0.04$ and $\alpha = 0.02$ [Fig.6(b)] and increases in time, what eventually has less impact on phase perturbation in \bar{x} oscillations in upper layer. The inset in Fig.6(a) shows that, the density flow between layers for first few oscillations of \bar{x} lowers only the amplitude of oscillations but motions of the upper and lower densi-

ties remain synchronous. But when the amplitude gets smaller for $t > 100$ ps, electron slows down what in consequence lowers the magnitude of magnetic force and for certain time period dumps the density flow between layers [compare the amplitudes of $\langle \rho \rangle$ at left and right sides in Fig.6(b)]. After that, the coupling between upper and lower densities raises, both densities oscillate coherently what eventually makes the amplitude of \bar{x} to grow. This periodic coupling and decoupling of both densities lead eventually to formation of beating pattern in $\bar{x}(t)$ function if an electron is allowed to oscillate in nanowire for longer times [Fig.6(a)]. Similar beating pattern for \bar{x} oscillations we also notice in Fig.6(c) for larger effective mass of an electron i.e. for $m^* = 0.067$. In this case, only a small asymmetry in a confining potential ($\alpha = 0.005$) is required to localize about 70% of total electron density in upper layer. Unlike the previous case, now the motions of both parts of electron wavepacket are decoupled for any time instant because as we see in Fig.6(c), the oscillations of density in lower layer exhibit, to some extent, a chaotic behaviour. Besides the fact, the density may still flow between layers [see Fig.6(d)], this chaotic motion of density in lower layer does not perturb the frequency of \bar{x} oscillations in upper layer but it influences their amplitude.

In the last part of this section we present the results of simulations performed for the pulse being formed when the magnetic field is switch off [$\beta = 1$ and $\gamma = 0$ in Eq.7]. Present case is different from that considered in Sec.III A since now, the electron wavepacket is prepared at $t = 0$ for $B > 0$ what means the densities confined in layers are magnetically coupled at the beginning of simulation and their spatial localizations in vertical direction are lowered when magnetic field vanishes in time. Results for $m^* = 0.04$ are presented in Fig.7. Unlike the preceding case with magnetic field growing in time and being fixed afterwards, here we have $B = 0$ for $t > t_{imp}$ what implies the lack of an electron density flow between layers then. Since the magnetic force is absent for $t > t_{imp}$, densities in both layers oscillate coherently along the wire axis and the pattern of \bar{x} does not change in time of simulation i.e. the period of oscillations is fixed [cf. Figs. 7(a) and 7(c)]. The degree of asymmetry in vertical confinement has large impact on sensitivity of the system on a time length of magnetic pulse. For slightly asymmetric confinement ($\alpha = 0.005$) the amplitude of \bar{x} in upper layer is slowly diminishing as t_{imp} grows. For larger asymmetry ($\alpha = 0.02$), the amplitude of \bar{x} gets smaller rapidly for $t_{imp} > 12$ ps. This qualitative difference in amplitude of oscillations of an electron position obviously stems from the different dynamics of the electron density in layers for $t < t_{imp}$ that is when the layers are magnetically coupled through the non-vanishing off-diagonal elements in Hamiltonian 2. We will analyze this difference for $t_{imp} = 12$ ps for which the time variations of $\langle \rho \rangle$ and \bar{x} are shown in Figs. 7(b,e) and 7(c,f), respectively. In Fig.7(b) we notice that for $\alpha = 0.005$ about 80% of electron density is localized in upper layer at $t = 0$. When

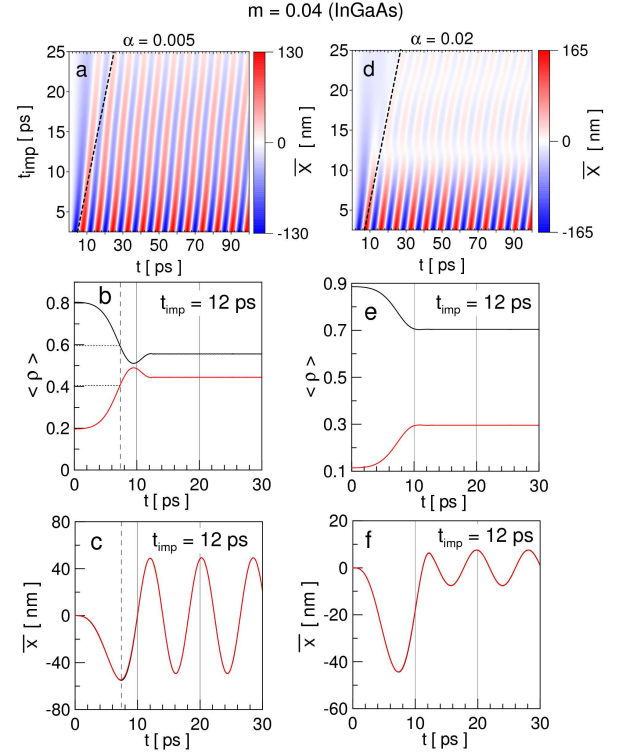


FIG. 7: (Color online) (a,d) Dependence of \bar{x} on the time length of magnetic pulse and on the time of simulation for a case the magnetic field is switched off [$\partial B / \partial t < 0$ for $t < t_{imp}$ and $B = 0$ for $t > t_{imp}$]. (b,e) The time changes of densities gathered in upper layer (black color) and in lower layer (red color). (c,f) The normalized expectation value of electron position in upper (black color) and in lower (red color) layers - they are the same. The results showed in first and in second column were obtained for $\alpha = 0.005$ and $\alpha = 0.02$, respectively.

the magnetic field is getting smaller, the electric field generated in bi-layer wire pushes an upper, majority part of density to the left what drags the lower one in this direction too. Both densities start to move coherently [see Fig.7(c)]. However, since the magnetic field becomes weaker, the density is no longer strongly squeezed in upper layer and it starts to flow to lower layer what is additionally enhanced by the magnetic force which is directed downwards. At $t = 7.4$ ps, when the upper and lower densities are turned back, as large as 20% of total density has been transferred to the lower layer. After reversing the direction of velocity of an electron, the lower part of wavepacket is now accelerated by electric field while the upper part is decelerated by it. For this reason, the density still flows from an upper layer to a lower one until it is almost equally distributed [$\langle \rho \rangle_u = 0.51$ and $\langle \rho \rangle_l = 0.49$] for $t = 9.5$ ps [see Fig.7(b)] what takes place just before the electron will pass the center of a wire [cf. Figs. 7(b) and 7(c) for $t = 0$]. In next two picoseconds, the direction of density flow is reversed, and when the magnetic field is finally turned off about 56% of total density is

localized in upper layer and 44% in lower one.

If distortion in vertical confinement is larger ($\alpha = 0.02$), even 90% of total density is gathered in upper layer at $t = 0$ and it drops to about 78% immediately it reaches the left turning point what one may notice in Fig.7(e). When the velocity of wavepacket is reversed, the majority part of density is strongly decelerated by an electric field what significantly diminishes the amplitude of oscillations of an electron position along the wire's axis [Fig.7(f)]. Therefore, we may conclude that for longer time intervals needed for switching the magnetic field off, the dynamics of the majority part of electron density for $\alpha = 0.02$ cannot adapt to the time scale of the magnetic pulse what in consequence prevents the electron from gaining the large values of \bar{x} [see Fig.7(d) for $t_{imp} > 12$ ps].

IV. CONCLUSIONS

The dynamics of an electron motion induced in quantum wire by a magnetic pulse was theoretically studied by means of computer simulations. We have shown that such motion can be realized in a semiconductor nanostructure which consist of two vertically stacked layers. If these layers are tunnel coupled then the wave functions associated with two lowest bounding and antibounding eigenstates for direction being perpendicular to both, the wire's axis and layers, can be easily hybridized in magnetic field. In such case, the rotational electric field generated due to the Maxwell law by a non-zero time derivative of \vec{B} may accelerate the charge density localized in the upper and lower parts of bi-layer nanowire. For symmetric confinement in vertical direction, the upper and lower charge densities are forced to move always in opposite directions according to the local directions of the electric field. However, it was proven that the electron wavepacket, as a whole, can be accelerated in arbitrarily chosen direction if the confinement in upper and in lower layers becomes asymmetric. Then, the majority part of charge density localized in one layer is pushed by the electric field and it simultaneously drags the minor part

in the same direction against the electric field generated in second layer. The dynamics of an electron wavepacket becomes thus dependent on effective mass of an electron, degree of asymmetry in the confining potential as well as on the time characteristics of the magnetic pulse. It was found that generally only the short time magnetic pulses with time duration of about several to maximally a few tens of picoseconds may significantly change the motion energy of an electron. Moreover, the coherent motion of both the upper and lower parts of wavepacket in the same direction can be realized only if the magnetic coupling between layers vanishes when the magnetic pulse is ended. This takes place when a single magnetic pulse is applied to the system or a magnetic field is switched off. In the opposite case, the magnetic force constantly changes the amounts of densities confined within layers what destroys their coherent motion in a nanowire.

We think that discussed here the effect of temporary change of electron's motion energy by picoseconds magnetic pulses can successfully be applied to the nanostructures consisting of two tunnel coupled wires allowing e.g. to sample the dynamical properties of many-body interactions¹⁵ including the Wigner crystals.¹⁶ Moreover, this effect can be also utilized in the nanostructures holding a two-dimensional electron gas within the single, wide quantum well established in growth direction⁷, allowing for studies of the dynamical properties of electron transport in QPC^{17,18} or temporary changes in the local potential landscape in conjunction with external biased gates.¹⁷

Acknowledgements

The work was financed by Polish Ministry of Science and Higher Education (MNiSW)

References

-
- * Electronic address: chwiej@fis.agh.edu.pl
- ¹ C. C. Eugster and J. A. del Alamo, *Phys. Rev. Lett.* **67**, 3586 (1991).
 - ² O. Bierwagen, C. Walther, W. T. Masselink, and K.-J. Friedland, *Phys. Rev. B* **67**, 195331 (2003).
 - ³ S. K. Lyo, *J. Phys.: Condens. Matter* **8**, L703 (1996).
 - ⁴ L. G. Mouroukh, A. Y. Smirnov, and S. F. Fischer, *Appl. Phys. Lett.* **90**, 132108 (2007).
 - ⁵ S. F. Fischer, G. Apetrii, U. Kunze, D. Schuh, and G. Abstreiter, *Phys. Rev. B* **74**, 115324 (2006).
 - ⁶ D. Huang, S. K. Lyo, K. J. Thomas, and M. Pepper, *Phys. Rev. B* **77**, 085320 (2008).
 - ⁷ S. F. Fischer, G. Apetrii, U. Kunze, D. Schuh, and G. Abstreiter, *Phys. Rev. B* **71**, 195330 (2005).
 - ⁸ K. J. Thomas, J. T. Nicholls, M. Y. Simmons, W. R. Tribe, A. G. Davies, and M. Pepper, *Phys. Rev. B* **59**, 12252 (1999).
 - ⁹ J.-R. Shi and B.-Y. Gu, *Phys. Rev. B* **55**, 9941 (1997).
 - ¹⁰ T. Chwiej, *Physica E* **77**, 169 (2016).
 - ¹¹ D. H. Auston, *Appl. Phys. Lett.* **26**, 101 (1975).
 - ¹² Z. Wang, M. Pietz, J. Walowski, A. Förster, M. I. Lepsa, and M. Münzenberg, *J. Appl. Phys.* **103**, 123905 (2008).
 - ¹³ C. Vicario, C. Ruchert, F. Ardana-Lamas, P. M. Derlet, B. Tudu, L. J., and C. P. Hauri, *Nat. Photon.* **7**, 720 (2013).
 - ¹⁴ T. Chwiej, arXiv.org (2015), URL

- <http://http://arxiv.org/abs/1508.05793v1>.
- ¹⁵ S. Kumar, K. J. Thomas, L. W. Smith, M. Pepper, G. L. Creeth, I. Farrer, D. Ritchie, G. Jones, and J. Griffiths, Phys. Rev. B **90**, 201304 (2014).
- ¹⁶ M. Yamamoto, H. Takagi, M. Stopa, and S. Tarucha, Phys. Rev. B **85**, 041308 (2012).
- ¹⁷ S. Schnez, C. Rössler, T. Ihn, K. Ensslin, C. Reichl, and W. Wegscheider, Phys. Rev. B **84**, 195322 (2011).
- ¹⁸ S. Baer, C. Rössler, E. C. de Wiljes, P.-L. Ardel, T. Ihn, K. Ensslin, C. Reichl, and W. Wegscheider, Phys. Rev. B **89**, 085424 (2014).